View metadata, citation and similar papers at core.ac.uk

brought to you by CORE

provided by Open Archive Toulouse Archive Ouverte

Open Archive TOULOUSE Archive Ouverte (OATAO)

OATAO is an open access repository that collects the work of Toulouse researchers and makes it freely available over the web where possible.

This is an author-deposited version published in : http://oatao.univ-toulouse.fr/
Eprints ID : 18163

To link to this article : DOI: 10.1080/10255842.2016.1143464
URL : http://dx.doi.org/10.1080/10255842.2016.1143464

To cite this version : Yang, J. and Faverjon, B. and Dureisseix, David and Swider, Pascal and Kessissoglou, N. *Prediction of the intramembranous tissue formation during perisprosthetic healing with uncertainties. Part 1. Effect of the variability of each biochemical factor.* (2016) Computer Methods in Biomechanics and Biomedical Engineering, vol. 19 (n° 13). pp. 1378-1386. ISSN 1025-5842

Any correspondence concerning this service should be sent to the repository administrator: staff-oatao@listes-diff.inp-toulouse.fr

Prediction of the intramembranous tissue formation during perisprosthetic healing with uncertainties. Part 1. Effect of the variability of each biochemical factor

J. Yang[a], B. Faverjon[a,b], D. Dureisseix[b], P. Swider[c] and N. Kessissoglou[a]

[a]School of Mechanical and Manufacturing Engineering, UNSW Australia, Sydney, Australia; [b]Université de Lyon, CNRS, INSA-Lyon, France; [c]Université de Toulouse, CNRS, INP-Toulouse, France

ABSTRACT

A stochastic model is proposed to predict the intramembranous process in periprosthetic healing in the early post-operative period. The methodology was validated by a canine experimental model. In this first part, the effects of each individual uncertain biochemical factor on the bone-implant healing are examined, including the coefficient of osteoid synthesis, the coefficients of haptotactic and chemotactic migration of osteoblastic population and the radius of the drill hole. A multi-phase reactive model solved by an explicit finite difference scheme is combined with the polynomial chaos expansion to solve the stochastic system. In the second part, combined biochemical factors are considered to study a real configuration of clinical acts.

KEYWORDS

Implant fixation; stochastic model; polynomial chaos expansion; biomechanics

1. Introduction

The primary fixation of an orthopedic implant greatly affects its clinical longevity (Albrektsson et al. 1983; Hahn et al. 1988). The periprostheic tissue healing is influenced by a significant number of factors including the patients clinical condition (Colnot et al. 2007), the mechano-chemico-bio factors (Colnot et al. 2007) and the surgical technique (Morshed et al. 2007). Low performance of implant fixation is generally associated with a low mineralization or a heterogeneous ossification of new-formed tissue (Morshed et al. 2007; Schwarz et al. 2007) but conditions favouring the healing process in the early post-operative period remain a clinical concern. The bone structure can be represented at the mesoscopic scale by a biphasic medium including a porous skeleton drained by the bone marrow and the vascularization. The intramembranous healing involves the osteoblast population, which proliferates and migrates in the marrow in the presence of growth factors. The osteoblast cells promote bone formation and mineralization by depositing new bone tissue on the implant surface and surrounding bone (Davies 2003). The growth factors regulate cell proliferation and stimulate bone matrix formation (Conover 2000) in the presence of mechanical factors coming from the implant design and joint loads (Babiker et al. 2013). Early numerical models of a bone healing process were based on pure mechanical approaches and focused on the mechanical behaviour while simplifying the biochemical and time effects (Carter et al. 1988; Viceconti et al. 2000). Numerical models have also been developed to examine the biological and transient behaviours of the cells and growth factors. Biomathematical models of migration and differentiation have been proposed in skin and fracture healing (Tranqui and Tracqui 2000; Puthumanapully et al. 2008). Mechano-bioregulatory models that incorporated the angiogenesis and cell migration effects have been mainly concerned with the modelling of endochondral ossification processes (Geris et al. 2008). Numerical predictions have rarely been correlated to *in vivo* or *ex vivo* data, explicitly. The models initially proposed by Ambard et al. (2004) and Ambard and Swider (2006) combined poromechanics with computational cell biology while considering the biological tissue as a multiphasic reactive medium in the case of intramembranous healing. The methodology was supported by ex-vivo data from canine implant models (Søballe et al. 1992; Vestermark et al. 2004). Mechano-biochemical models are affected by significant uncertainties from the mechanical and biochemical environments and their influence becomes crucial given the high degree of non-linearities in coupling effects between mechanical governing equations and chemico-biological reactive sources. Models of uncertainty are generally based on either a parametric or a non-parametric description of the uncertainty. For a non-parametric analysis, uncertainties in the system are described using a universal model regardless

of their detailed nature, such as using the entropy optimization principle (Soize 2000) and random matrix theory (Kessissoglou and Lucas 2009). For a parametric description of uncertainty, random quantities are described using various techniques, including the Monte Carlo simulations (MCS) (Fishman 1995), perturbation method (Adhikari and Manohar 1999), random factor method (Gao and Kessissoglou 2007) and polynomial chaos expansion method (PCE) (Ghanem and Spanos 1991). The influence of uncertainties can be observed directly using MCS, which generate a large number of samples to obtain statistics of the output. Compared with MCS, the PCE can obtain the statistical characteristics of the results with greatly reduced computational cost. It has been successfully applied in a range of problems with uncertainties involving acoustics (Faverjon and Ghanem 2006) and fluid flow in porous media (Rupert and Miller 2007). We hypothesize that the PCE could be of great interest to identify the role of complex biochemical parameters involved in periprosthetic healing. This paper investigates the effects of uncertain biochemical parameters on the bone-implant healing process using the PCE methodology. The model considers coupled equations to take into account the osteoblast cells migration, growth factors diffusion and bone deposit. Results from the numerical model of the homogeneous healing of the bone implant are compared to canine experiments from literature (Vestermark et al. 2004). The explicit finite difference scheme is combined with the PCE to solve the stochastic system equations. Results are compared with MCS, showing good agreement with significantly reduced computational cost. In the first part of the paper, the relevance of the proposed methodology is established and the effects of the individual biochemical factors, corresponding to the coefficients of osteoid synthesis, haptotactic and chemotactic migrations on the solid fraction distribution in the neo-formed tissue are reported. Uncertainty in the drill hole radius on the bone-implant healing is also examined, which depends on the surgical technique. In the second part of the paper, the effects of these combined factors on the periprosthetic healing in the early post-operative period are examined.

2. Bone-implant healing model

2.1. Presentation of the tissue formation problem

Figure 1 shows a schematic diagram of the canine experimental implant previously examined *in vivo* (Vestermark et al. 2004). The studied experimental device is a stable implant. The pistoning system is not in contact with the tibia plateau. Therefore, no mechanical loading is applied on the implant during the healing time course. Boundary conditions and tissue formation showed a polar symmetry with a variable level of calcification (or mineralization) ϕ^s in the radial direction r. The peripheral domain denoted by r_s was the host trabecular bone. The intermediate domain bounded by the implant radius r_i and the drill hole radius r_d corresponded to the immediate post-operative gap. The healing process is evaluated up to 8 weeks post-operatively starting from the initial continuous distribution of the solid fraction $\phi^s_{\text{in}}(r)$ described by Equation (1) involving the transition distance δ_d, and properties at the implant surface $\phi^s_{r_i}$ and at the host bone $\phi^s_{r_s}$. The transition distance δ_d is a geometrical parameter that allowed regulating the transition between the very low initial structural fraction into the initial gap in the vicinity of the implant and the existing structural fraction of the host bone. Fluid flux, cell flux and growth factor flux were nil at boundaries.

$$\phi^s_{\text{in}}(r) = \frac{1}{2}\left(\phi^s_{r_s} + \phi^s_{r_i}\right) + \frac{1}{\pi}\left(\phi^s_{r_s} - \phi^s_{r_i}\right)\tan^{-1}\left[\frac{1}{\delta_d}\left(r - r_d\right)\right] \quad (1)$$

The set of convective-diffusive-reactive Equations (2)–(4) were obtained assuming incompressible phases in isothermal behaviour with no substrate strain (Ambard and Swider 2006). The model outputs were the evolving solid fraction ϕ^s (or the effective porosity $\phi^f = 1 - \phi^s$) of neo-formed tissue, the relative fluid flow rate $\mathbf{q}^f$ and the species concentrations: C^c and C^M for osteoblast population and growth factor phase, respectively.

$$\frac{\partial \phi^s}{\partial t} = \alpha^s {\phi^f}^2 C^c C^M = -\text{div}\mathbf{q}^f \quad (2)$$

$$\frac{\partial\left(\phi^f C^c\right)}{\partial t} = \text{div}\mathbf{q}^c + \alpha^c \phi^f C^c \left(N^{cc} - \phi^f C^c\right) \quad (3)$$

$$\frac{\partial\left(\phi^f C^M\right)}{\partial t} = \text{div}\mathbf{q}^M \quad (4)$$

with

$$\mathbf{q}^c = \phi^f\left(D^c \mathbf{grad} C^c - h^c \rho^s C^c \mathbf{grad}\phi^s - \chi^c C^c \mathbf{grad} C^M\right)$$
$$\mathbf{q}^M = D^M \phi^f \mathbf{grad} C^M + C^M \mathbf{q}^f$$

where α^s, h^c, χ^c and α^c are respectively the coefficients of osteoid synthesis, haptotactic migration, chemotactic migration and cell proliferation. $\mathbf{q}^c$ and $\mathbf{q}^M$ are respectively the cell and the growth factors flow rates. D^c and D^M are respectively the coefficients of cell and growth factors diffusion. N^{cc} is the inhibition level of cell proliferation, which is the maximum concentration of cell per volume unit, and ρ^s is the density of solid phase. The active migrations of osteoblast population involved chemotaxis and haptotaxis processes, and neo-formation of tissue

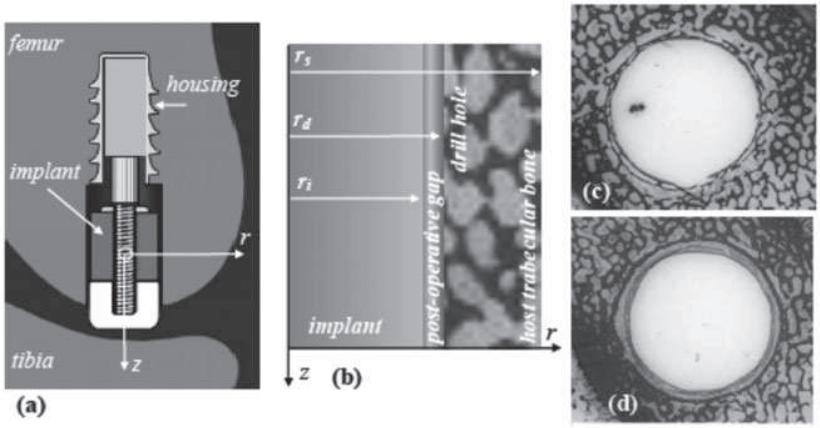

Figure 1. Canine experimental model: (a) implant diagram; (b) implant parameterization; and histological results for reference: (c) GH, (d) PH.

were taken into account by source terms. The coefficient of osteoid synthesis α^s shows that the solid matrix source is proportional to the concentration of osteoblast cells C^c and growth factors C^M (Linkhart et al. 1996). Haptotactic flow is proportional to the solid fraction gradient and chemotactic flow is proportional to the growth factors gradient (Friedl et al. 1998).

Two main classes of results were distinguished by the average level of solid fraction ϕ^s. The spatial–temporal evolution of this fraction revealed the biological activity of osteoblast population in term of migration, proliferation, and synthesis of extra-cellular matrix that corresponded with the amount of calcified tissue per volume element. Two typical healing patterns encountered in the canine experiment were selected to support the computational developments. They were classified according to the amount of the solid fraction and designated as good healing (GH) when the average solid fraction was in the range of that of the host bone and poor healing (PH) for significantly lower values. Data associated with GH and PH are listed in Table 1. The concentration of growth factors in the host site is negligible compare to the one induced by a significant bleeding followed by the inflammation and therefore is fixed to 0. Common parameters for both healing patterns are $\delta_d = 0.1\,\text{mm}$, $N^{cc} = 1000\,\text{cell/mm}^3$, $\alpha^c = 1.9 \times 10^{-10}\,\text{mm}^3/\text{cell.s}$, $D^c = 2.5 \times 10^7\,\text{mm}^2/\text{s}$, $D^M = 4.8 \times 10^{-6}\,\text{mm}^2/\text{s}$, $\rho^s = 2.57 \times 10^{-6}\,\text{kg/mm}^3$, $r_i = 3.25\,\text{mm}$, $r_d = 4.1\,\text{mm}$, $r_s = 7\,\text{mm}$.

2.2. Stochastic modelling for the periprosthetic healing

Parameters were selected to include the most significant uncertainties. The drill hole radius r_d is dependent upon the surgical technique and consequently conditions the initial solid fraction ϕ^s_{in} (see Equation (1)). Three biochemical factors were examined, namely the coefficient of osteoid synthesis α^s, and the coefficients of haptotactic h^c and chemotactic χ^c migrations.

Using PCE, all biochemical factors, the initial solid fraction and the output quantities corresponding to the solid fraction ϕ^s, the porosity ϕ^f, the fluid flow $\mathbf{q}^f$, the cell concentration C^c and the growth factor concentration C^M can be expanded in a set of mutually orthogonal base polynomials Ψ_i, which are functions of an n-dimensional random variable $\boldsymbol{\xi} = \{\xi_1, \xi_2, \ldots, \xi_n\}$, such as Y given by Ghanem and Spanos (1991)

$$Y(\boldsymbol{\xi}) = \sum_{i=0}^{\infty} Y_i \Psi_i(\boldsymbol{\xi}) \tag{5}$$

where Y_i are deterministic coefficients. Practically, the summation is truncated to a limited number of base polynomials N. Hence Y can be approximated by

$$Y(\boldsymbol{\xi}) = \sum_{i=0}^{N} Y_i \Psi_i(\boldsymbol{\xi}) \tag{6}$$

The truncation N and the values of Y_i for the input data depend on the choice of variability of the model. The truncation for the output is obtained from the convergence of the solution. In Equation (6), the truncation N corresponds to N_α, N_h, N_χ, N_{ϕ_0} for α^s, h^c, χ^c and ϕ^s_{in}, respectively, and N_ϕ, N_q, N_c, N_M for the output quantities ϕ^s, ϕ^f, $\mathbf{q}^f$, C^c and C^M, respectively.

The intrusive PCE method is used in this first part of the paper as it is well adapted to a problem with one random variable since it provides good accuracy and is computationally fast, especially for non linear problems

Table 1. Parameters of the numerical model for the cases of PH and GH.

Parameter	New-formed tissue $r \in [r_i, r_d]$		Host trabecular bone $r \in [r_d, r_s]$	
	PH	GH	PH	GH
ϕ^s_{in} (%)	6	6	40	50
C^c_0 (cell.mm^{-3})	0	1064	1667	2000
C^M_0 (ng.mm^{-3})	0.2	0.2	0	0
α^s (mm^6.cell^{-1}.ng^{-1}.s^{-1})	3.25×10^{-9}	3.5×10^{-9}	3.25×10^{-9}	3.5×10^{-9}
h^c (mm^5.kg^{-1}.s^{-1})	0.78	0.7	0.78	0.7
χ^c (mm^5.ng^{-1}.s^{-1})	2×10^{-5}	7×10^{-5}	2×10^{-5}	7×10^{-5}

(Didier et al. 2013). The method consists in substituting PCE of the eight parameters above into the governing equations given by Equations (2)–(4) and into the initial solid fraction of Equation (1). Then, multiplying these equations by a base polynomial and using the Galerkin projection with the orthogonal relationship (Xiu and Karniadakis 2002) results in the set of deterministic equations for the one-dimensional radial axisymmetric bone implant. To solve the partial differential equations, the explicit finite difference scheme with variable time steps and upwinding was utilized. In the PCE framework, each single explicit finite difference equation was transformed to a set of equations, whose size depends on the PCE order.

3. Effect of the variability of individual factor in the solid fraction

The effects of single uncertainties in four model parameters on the solid fraction ϕ^s in neo-formed tissues were investigated. It concerned three biochemical factors: the coefficient of osteoid synthesis α^s, the coefficient of chemotactic migration χ^c, the coefficient of haptotactic migration h^c and a parameter associated with the surgical technique, namely the drill hole radius r_d. The histomorphometry is reproduced from Ambard and Swider (2006) and is used as a reference in the following results. Good tissue healing was characterized by the maximum value between 70 and 80% at the implant surface r_i and at the drill hole r_d showing increased biological activities in these zones. Poor tissue healing maintained a significant consolidation at the drill hole (60%) but showed a fast decay to the implant.

All random biochemical factors follow a uniform distribution within ranges given in Table 1 and are well represented by the first order Legendre PCE ($N_\alpha = N_h = N_\chi = 1$). The statistical moments of the solid fraction distribution, mean and variance, were obtained from the coefficients of PCE by $E[\phi^s] = \phi^s_0$ and $\sigma^2[\phi^s] = \sum_{i=1}^{N_\phi} \phi^{s2}_i E[\Psi^2_i]$ respectively. Envelopes of the maximum and minimum values of ϕ^s were constructed from its PCE representation using 50,000 samples.

3.1. Influence of coefficient of osteoid synthesis α^s

Variability in α^s was within the range $[1, 5] \times 10^{-9}$ mm^6/cell.ng.s. For a converged result, the number of base polynomial was $N_\phi = 2$ for ϕ^s. Figure 2(a) and (b) present the mean solid fraction and its variance for periprosthetic healing with GH and PH, respectively. Similar tendencies were obtained into the host bone ($r \in [r_d, r_s]$) in terms of mean values and variance of ϕ^s whereas the synthesis of osteoid tissue was more significant in the vicinity of the implant ($r \in [r_i, r_d]$) for the case of GH.

3.2. Influence of coefficient of haptotactic migration h^c

Coefficient of haptotactic migration h^c varied in the range $[4, 80] \times 10^{-2}$ mm^5/kg.s. Solid fraction was represented accurately by PCE order $N_\phi = 2$. Figure 3(a) and (b) show the mean and variance of ϕ^s for the GH and PH. Even if haptotaxis influenced the two groups of distribution patterns, the mean value associated with the variance in Figure 3(b) showed that the healing process was more affected by the uncertain h^c in the case of low-level mineralization. In both cases, the drill hole zone ($r = r_d$) was the location of significant disturbances.

3.3. Influence of coefficient of chemotactic migration χ^c

Variability in χ^c was assumed to be within $[1, 14.5] \times 10^{-5}$ mm^5/ng.s. For converged results, the third order Legendre PCE was chosen to represent the uncertain solid fraction distribution. As previously, the GH and PH were examined and corresponding results are presented in Figure 4(a) and (b), respectively. Two cases of healing patterns showed a significant sensitivity to χ^c in the zone of neo-formed tissue ($r \in [r_i, r_d]$). Due to the local concentration of growth factors, which drove the chemotactic flux, the mean values at the implant radius were impacted significantly. The chemotaxis showed a significant influence on the inhomogeneity of ϕ^s especially in the case of low calcification where the variance reached maximum values as shown in Figure 4(b).

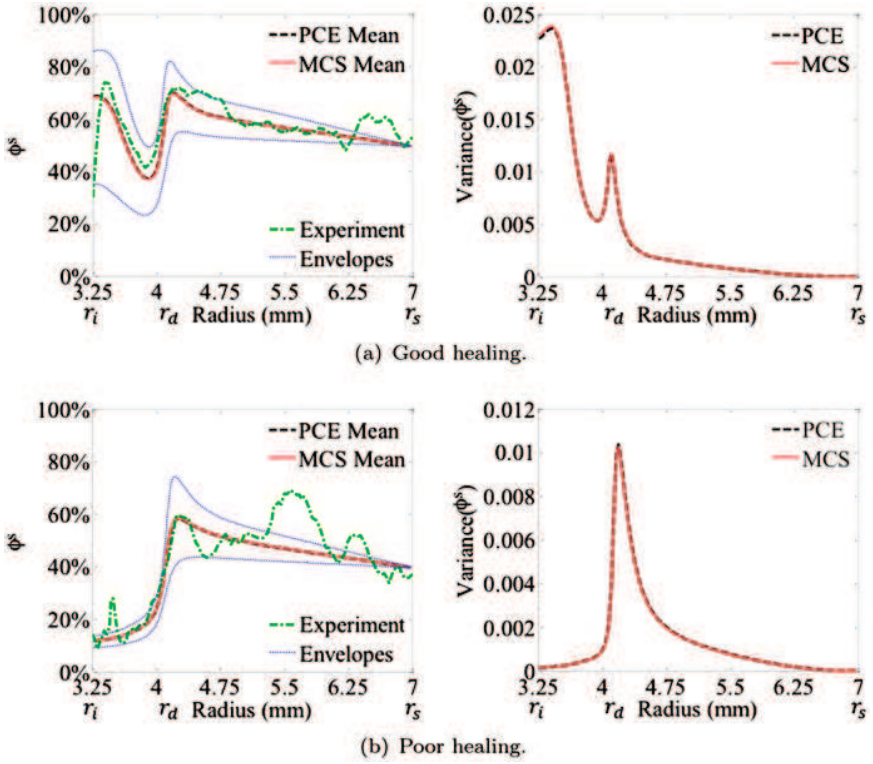

Figure 2. Statistics of solid fraction distribution ϕ^s with random osteoid synthesis α^s.

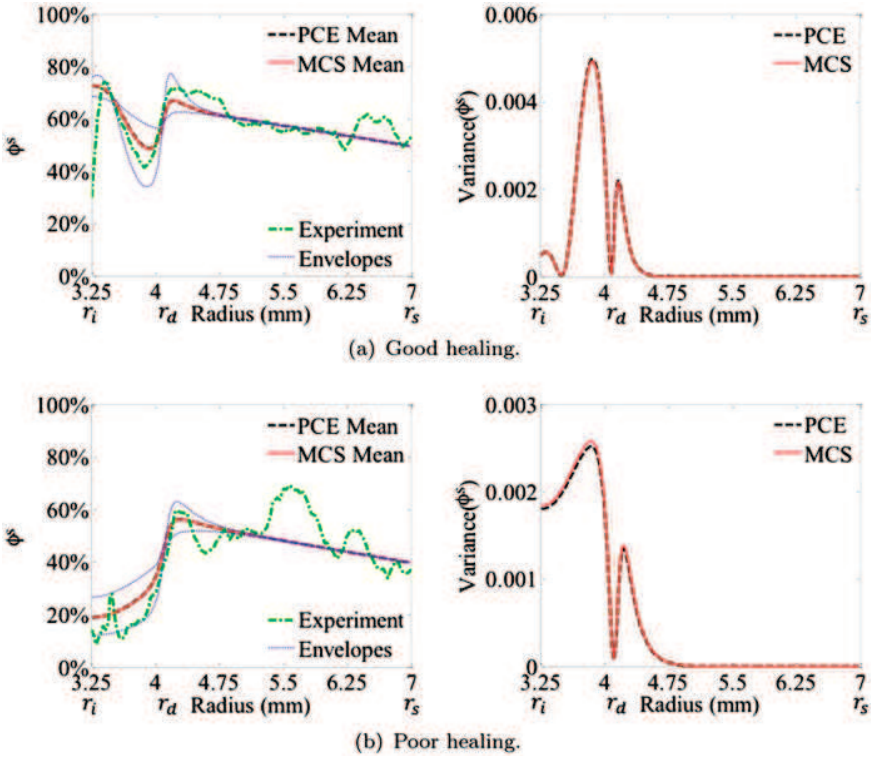

Figure 3. Statistics of solid fraction distribution ϕ^s with random haptotactic migration h^c.

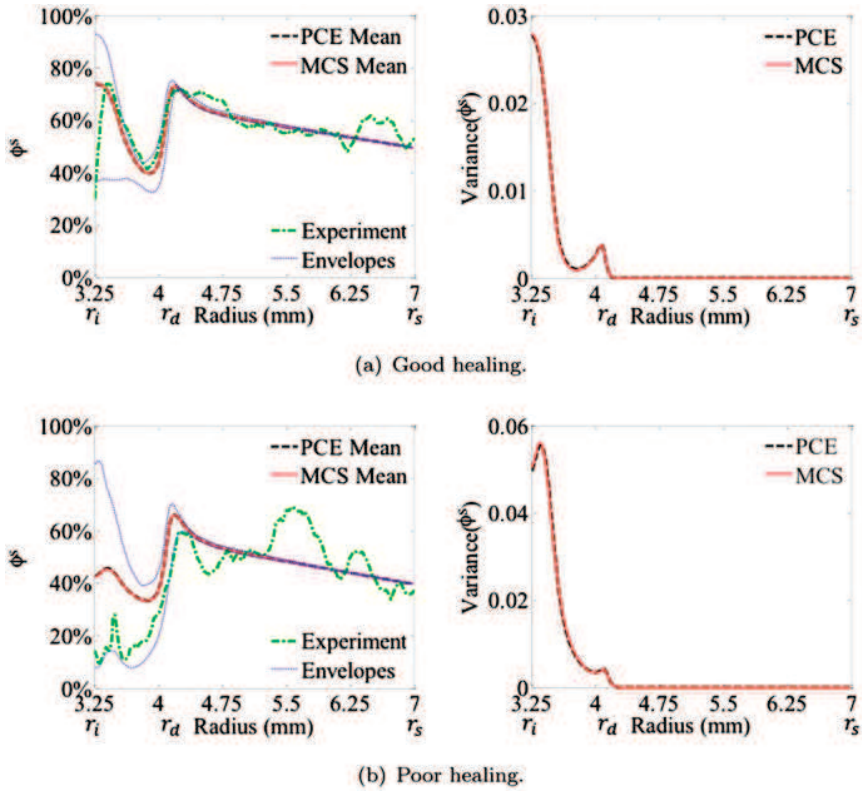

Figure 4. Statistics of solid fraction distribution ϕ^s with random chemotactic migration χ^c.

3.4. *Influence of the drill hole radius r_d*

The radius of the drill hole r_d was 4.1 ± 0.3 mm. According to Equation (1), uncertainty in r_d resulted in a random initial distribution of the solid fraction ϕ^s_{in}. Both ϕ^s_{in} and ϕ^s were represented by the third order Legendre PCE ($N_{\phi_0} = 3, N_\phi = 3$). The output measures are presented in Figure 5(a) and (b). The two cases of healing processes were affected by uncertainty of the drill hole radius. It was found that magnitude of ϕ^s was particularly evolving for the GH (Figure 5(a)) whereas that of the fraction of PH remained low (Figure 5(b)). This was corroborated by the variances showing significant fluctuations, which also confirmed that the amount of calcified tissue in the drill hole environment was particularly dependent on r_d.

3.5. *Discussion*

As shown in Figure 2–5 for the cases of GH and PH and individual parameters α^s, χ^c, h^s and r_d, results obtained by using PCE were in excellent agreement with MCS using 5000 samples with a saving in computational cost between 45 and 85%. Ex-vivo histological data from Ambard and Swider (2006) were added and comparison with predicted results was comforting considering the complexity of the biological mechanisms involved. Comparing Figure 2(a) and (b) showed that the osteoid synthesis driven by α^s had an impact at r_i and at the drill-hole r_d for GH and only at r_d for PH. In comparison, the haptotactic coefficient h^c showed less effect even if it influenced the homogeneity of structural fraction into the post-operative gap especially for GH (Figure 3(a)). The chemotactic coefficient χ^c played a significant role in tissue formation with a peak at r_i for both GH and PH as shown in Figure 4(a) and (b). For PH, we noted that the experimental results were close to the lower limit of the PCE envelope PCE. Figure 5 showed that the variations of r_d had a significant impact on the tissue formation at the drill hole and it modified the homogeneity of neo-formed tissue in the gap $r_i - r_d$ especially for GH. The stochastic modelling aims to show the variability of selected parameters of the theoretical model on the predicted response. Direct effect and coupled effects are predicted. In that sense, it constitutes an elegant and powerful approach. It helps predicting the variety of response and while doing this it helps to understand and interpret the complex mechanisms involved into the perisprosthetic implant healing.

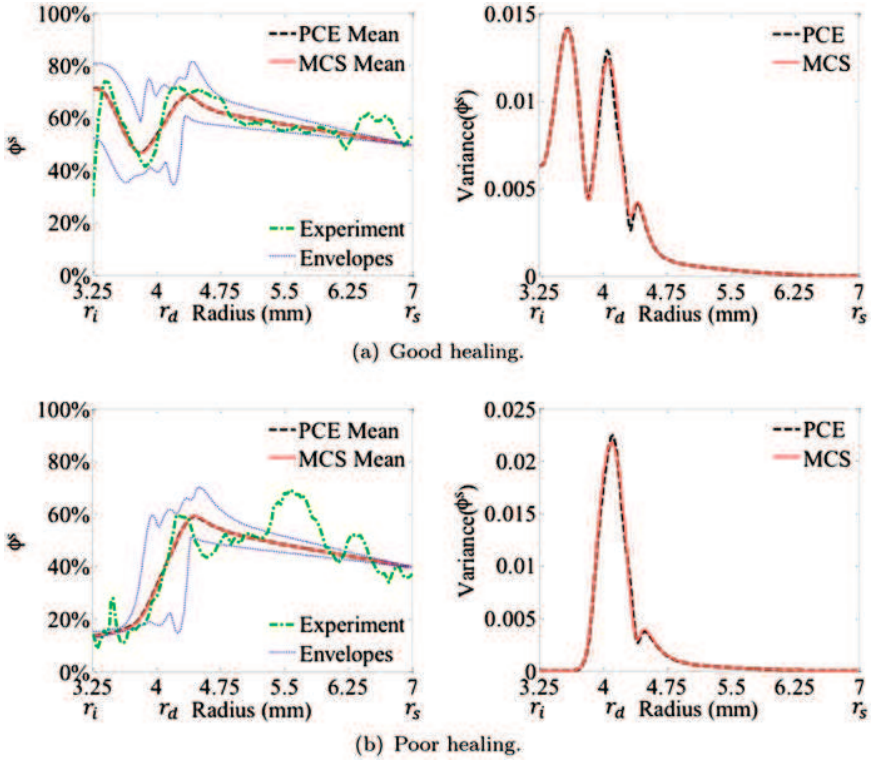

Figure 5. Statistics of solid fraction distribution ϕ^s with random radius of drill hole r_d.

4. Conclusions

PCE was demonstrated to be of great interest to explore biological events involved in the early post-operative healing of periprosthetic tissue. A stochastic formulation was obtained from the combination of reactive equations with PCE, and was applied to an experimental canine implant. The output data was the distribution of the structural (or calcified) fraction of neo-formed tissue that reveals the quality of the primary fixation and condition of its long-term behaviour. The intramembranous healing is complex and multifactorial. As a first step, the most significant factors were individually examined, including three biochemical factors and one parameter related to the surgical technique. The analysis of mean values, variances and envelopes provided new insights for the interpretation. Compared with MCS, the stochastic model was shown to provide accurate results with significantly reduced computational cost.

The PCE was able to describe the significant non-linearity provoked by the coupling effects in chemico-biological reactive sources. As observed in clinics, the osteoid synthesis is important in the vicinity of the implant because of the initial presence of cells, growth factors in the blood clot and bioactive coating. This also drove the chemotactic flux of cells towards the implant surface. The PCE order for the output structural fraction for this case was increased, showing greater nonlinear effects of uncertain chemotactic coefficient. The model also predicts a significant variance of structural fraction at the implant surface, which highlighted the role of implant bioactive coating observed in clinical results. The uncertain haptotactic coefficient had a lesser impact on the structural fraction even if it tended to provoke a bone condensation at the drill hole because of the porosity gradient in this zone, after the surgery. This healing pattern is corroborated by clinical results.

Finally, PCE allowed prediction of the role of the uncertain drill hole radius, which is a crucial issue *in vivo*. As confirmed in previous experimental work and in human arthroplasty, the surgical technique is operator dependent and it guides the quality of implant fixation. PCE results showed that the drill hole radius strongly influenced the homogeneity of the structural fraction and played a significant role on the variance of neo-formed bone in the drill hole zone. The PCE in general allowed prediction of the mean value of the structural fraction as well as its minimum and maximum values. The envelope results highlighted asymmetrical distribution patterns of boundaries, which confirms that the numerical method is able to depict the non-linear and biophysical events shown in experimental and clinical observations.

In conclusion, the PCE has been shown to be a powerful numerical method to predict and interpret nonlinear phenomena involved in the biological responses of biological tissue. The next step is to evaluate its capacity to explore the role of mechanical strain on the tissue biophysical response and in particular the influence of loading cycles and micromotions on the immediate post-operative periprosthetic healing, as well as its effectiveness in taking into account simultaneous sources of variability. This last issue is studied in the second part of the paper.

Acknowledgements

B. Faverjon gratefully acknowledges the French Education Ministry, University of Lyon, CNRS, INSA of Lyon and LabEx iMUST for the CRCT and the out mobility grant. The authors wish to thank J. E. Bechtold PhD (Departments of Orthopaedic Surgery, Mechanical and Biomedical Engineering, University of Minnesota USA) and K. Soballe MD, PhD (University Hospital of Aarhus, Denmark) for the experimental studies (NIH USA AR 42051).

Disclosure statement

No potential conflict of interest was reported by the authors.

Notes on contributors

Ji Yang is a PhD candidate in the University of New South Wales. His research is about the stochastic models of mechanical and biomedical structures.

Beatrice Faverjon is an associate professor in Mechanical Engineering at INSA Lyon/University of Lyon, France. Her research interest focuses on probabilistic modeling in vibration and biomechanics applications.

David Dureisseix is a professor at INSA Lyon/University of Lyon, France, and formerly head of the Contact and Structural Mechanics Laboratory (LaMCoS, INSA Lyon/CNRS UMR5259). His research interests lie in the computational mechanics field. He is more specifically involved in multiphysics and multiscale simulations, with high-performance computing and numerical strategies. Some specific topics include: homogenization, domain decomposition, partitioning strategies for coupled problems, frictional contact problems, and applications to biomechanics.

Pascal Swider is a full Professor in Toulouse University – France and he established an interdisciplinary research group in mechanobiology at Toulouse University Hospital. His research interest focuses on musculoskeletal pathologies (pediatric pathologies, aging pathologies, and oncology). He has published over 60 papers in international peer-reviewed journals.

Nicole Kessissoglou is an associate professor in the School of Mechanical and Manufacturing Engineering at UNSW Australia. She has published over 50 papers in international peer-reviewed journals.

References

Adhikari S, Manohar CS. 1999. Dynamic analysis of framed structures with statistical uncertainties. Int J Numer Methods Eng. 44(8):1157–1178.

Albrektsson T, Brånemark PI, Hansson HA, Kasemo B, Larsson K, Lundström I, McQueen DH, Skalak R. 1983. The interface zone of inorganic implants in vivo: titanium implants in bone. Ann Biomed Eng. 11(1):1–27.

Ambard D, Bechtold JE, Søballe K, Swider P. 2004. Prediction of the periprosthetic tissue mineralization of a stable implant coupling cell diffusion to porous media mechanics. 6th International Symposium on Computer Methods in Biomechanics and Biomedical Engineering. Madrid, Spain.

Ambard D, Swider P. 2006. A predictive mechano-biological model of the bone-implant healing. Eur J Mech A/Solids. 25:927–937.

Babiker H, Ding M, Overgaard S. 2013. Evaluating of bone healing around porous coated titanium implant and potential systematic bias on the traditional sampling method. J. Biomech. 46(8):1415–1419.

Carter DR, Blenman PR, Beaupré GS. 1988. Correlations between mechanical stress history and tissue differentiation in initial fracture healing. J Orthopaedic Res. 6(5):736–748.

Colnot C, Romero D, Huang S, Rahman J, Currey J, Nanci A, Brunski J, Helms J. 2007. Molecular analysis of healing at a bone-implant interface. J Dent Res. 86(9):862–867.

Conover CA. 2000. Insulin-like growth factors and the skeleton. Philadelphia (PA): Lippincott Williams & Wilkins; p. 101–116.

Davies J. 2003. Understanding peri-implant endosseous healing. J Dent Edu. 67(8):932–949.

Didier J, Sinou JJ, Faverjon B. 2013. Nonlinear vibrations of a mechanical system with non-regular nonlinearities and uncertainties. Commun Nonlinear Sci Numer Simul. 18(11):3250–3270.

Faverjon B, Ghanem R. 2006. Stochastic inversion in acoustic scattering. J Acoust Soc Am. 119(6):3577–3588.

Fishman GS. 1996. Monte carlo: concepts, algorithms, and applications. In: Peter Glynn, editor. Springer series in operations research. New York, Berlin: Springer.

Friedl P, Zänker KS, Bröcker EB. 1998. Cell migration strategies in 3-D extracellular matrix: differences in morphology, cell matrix interactions, and integrin function. Microsc Res Tech. 43(5):369–378.

Gao W, Kessissoglou N. 2007. Dynamic response analysis of stochastic truss structures under non-stationary random excitation using the random factor method. Comput Methods Appl Mechan Eng. 196(25–28):2765–2773.

Geris L, Gerisch A, Sloten JV, Weiner R, Oosterwyck HV. 2008. Angiogenesis in bone fracture healing: a bioregulatory model. J Theor Biol. 251(1):137–158.

Ghanem RG, Spanos PD. 1991. Stochastic finite elements: a spectral approach. New York: Springer-Verlag.

Hahn M, Vogel M, Eckstein F, Pompesius-Kempa M, Delling G. 1988. Bone structure changes in hip joint endoprosthesis implantation over the course of many years. A quantitative study. Chirurg. 59(11):782–787. German.

Kessissoglou NJ, Lucas GI. 2002. Gaussian orthogonal ensemble spacing statistics and the statistical overlap factor applied to dynamicsystems. Journal of Sound and Vibration. 324(3):1039–1066.

Linkhart TA, Mohan S, Baylink DJ. 1996. Growth factors for bone growth and repair: IGF, TGF beta and BMP. Bone. 19(1, Supplement 1):S1–S12. Proceedings of the Portland Bone Symposium 1995.

Morshed S, Bozic KJ, Ries M, Malchau H, Colford JJ. 2007. Comparison of cemented and uncemented fixation in total hip replacement: a meta-analysis. Acta Orthop. 78(3):315–26.

Puthumanapully P, New A, Browne M. 2008. Do multi-layer beads on porous coated implants influence bone ingrowth? A finite element study. J Biomech. 41:S290.

Rupert C, Miller C. 2007. An analysis of polynomial chaos approximations for modeling single-fluid-phase flow in porous medium systems. J Comput Phys. 226(2):2175–2205.

Schwarz F, Herten M, Sager M, Wieland M, Dard M, Becker J. 2007. Histological and immunohistochemical analysis of initial and early osseous integration at chemically modified and conventional sla titanium implants: preliminary results of a pilot study in dogs. Clin. Oral Implants Res. 18(4):481–488.

Søballe K, Hansen ES, B-Rasmussen H, Jørgensen PH, Bünger C. 1992. Tissue ingrowth into titanium and hydroxyapatite-coated implants during stable and unstable mechanical conditions. J Orthopaedic Res. 10(2):285–299.

Soize C, . 2000. A nonparametric model of random uncertainties for reduced matrix models in structural dynamics. Probabilistic Engineering Mechanics. 15(3):277–294.

Tranqui L, Tracqui P. 2000. Mechanical signalling and angiogenesis. The integration of cellextracellular matrix couplings. CR Acad Sci Ser III. 323(1):31–47.

Vestermark MT, Bechtold JE, Swider P, Søballe K. 2004. Mechanical interface conditions affect morphology and cellular activity of sclerotic bone rims forming around experimental loaded implants. J Orthopaedic Res. 22(3):647–652.

Viceconti M, Muccini R, Bernakiewicz M, Baleani M, Cristofolini L. 2000. Large-sliding contact elements accurately predict levels of boneimplant micromotion relevant to osseointegration. J Biomechan. 33(12):1611–1618.

Xiu D, Karniadakis GE. 2002. Wiener-askey polynomial chaos for stochastic differential equations. SIAM J Sci Comput. 24(2):619–644.